

RESEARCH ARTICLE OPEN ACCESS

Morphometric Evidence of a U-Shaped Relationship Between Loss Aversion and Posterior Insular/Somatosensory Cortical Features

Maria Arioli¹ | Letizia Richelli^{2,3} | Giulia Mattavelli^{2,3} | Zaira Cattaneo¹ | Paolo Poggi⁴ | Nicola Canessa^{2,3} 

¹Department of Human and Social Sciences, University of Bergamo, Bergamo, Italy | ²IUSS Cognitive Neuroscience (ICoN) Center, Scuola Universitaria Superiore IUSS, Pavia, Italy | ³Cognitive Neuroscience Laboratory of Pavia Institute, Istituti Clinici Scientifici Maugeri IRCCS, Pavia, Italy | ⁴Radiology Unit of Pavia Institute, Istituti Clinici Scientifici Maugeri IRCCS, Pavia, Italy

Correspondence: Nicola Canessa (nicola.canessa@iusspavia.it)

Received: 31 October 2024 | **Revised:** 29 April 2025 | **Accepted:** 17 June 2025

Funding: This work was supported by the “Ricerca Corrente” funding scheme of the Italian Ministry of Health to ICS Maugeri and “Dipartimenti di Eccellenza 2023–2027” funding scheme of the Italian Ministry of University and Research to IUSS Pavia.

Keywords: decision-making | interoception | intervention | loss aversion | posterior insula | surface-based morphometry | voxel-based morphometry

ABSTRACT

Neuroeconomic findings show that interoceptive sensitivity contributes to the typical overweighting of prospective losses over gains known as “loss aversion.” Whether the latter is related to the morphometric properties of the insula—a key node for interoception—remains, however, debated, due to previous conflicting evidence of both positive and negative correlations between their respective metrics. We combined a well-established behavioral modeling approach with a comprehensive morphometric protocol to explore both a linear and quadratic relationship between loss aversion and distinct voxel-based and surface-based cortical features in a sample of 208 healthy young individuals. Both univariate and multivariate analyses highlighted a positive quadratic (i.e., U-shaped) relationship between loss aversion and distinct morphometric features of the posterior insula and somatosensory-parietal cortex. These results first suggest that previous inconsistent findings might reflect methodological differences across studies, facilitating the detection of either the descending or ascending sectors of a U-shaped relationship between loss aversion and structural features. Moreover, they provide novel insights into the interoceptive modulation of choice-related evaluations guiding decision-making towards or away from loss avoidance, thus paving the way to studies investigating alterations of this mechanism in neuro-psychiatric conditions and its susceptibility to different types of intervention including neuromodulation.

1 | Introduction

The growth of neuroeconomics has gradually refined hypotheses on the neural modulators of decision-making and behavioral learning, from *somatic markers* engaging the ventromedial prefrontal cortex (vmPFC) amygdala and somatosensory/insular cortices (see Bechara 2000), to interoceptive representations of predicted *emotional and bodily states* (Berntson and Khalsa 2021). Neuroeconomic studies indeed highlighted

structures associated with interoception, such as orbitofrontal and medial prefrontal cortex (including anterior and midcingulate cortex), somatosensory cortex and insula (Berntson and Khalsa 2021; Serra 2021).

In particular, the insular cortex underpins different interoception processes (Chen et al. 2021; Wang et al. 2019) along its anterior (three or four “short” gyri) and posterior (two “long” gyri) subregions. The posterior insula encodes primary

This is an open access article under the terms of the [Creative Commons Attribution-NonCommercial-NoDerivs](https://creativecommons.org/licenses/by-nc-nd/4.0/) License, which permits use and distribution in any medium, provided the original work is properly cited, the use is non-commercial and no modifications or adaptations are made.

© 2025 The Author(s). *Human Brain Mapping* published by Wiley Periodicals LLC.

representations of afferent objective interoceptive inputs (e.g., visceral sensations) that are progressively integrated and re-represented—as *subjective* sensations—in the middle and then anterior, insula (Craig 2009a, 2009b, 2015). These findings first suggest that “somatic markers” (Bechara 2000) reflect neurophysiological processes whereby anticipated bodily states influence upcoming behavior (Tan et al. 2022). Alongside increasing evidence of the insular involvement in decision-making (Uddin et al. 2017), they also suggest a neural mechanism through which emotion-related signals shape decision-making patterns often labeled as “cognitive biases.” A prototypical example is loss aversion (LA), that is, the tendency to avoid losses more strongly than to pursue equivalent gains (Kahneman and Tversky 1979). LA is typically measured with mixed gambles offering 50% chances of gaining or losing different amounts (Arioli et al. 2023; Sokol-Hessner et al. 2009; Tom et al. 2007), with the overweighting of negative outcomes reflecting in a “lambda” (λ) parameter typically around 2 (1.820–2.102 in Brown et al.’s 2024 meta-analysis). Since choices in gain-loss trials are also shaped by risk attitudes (because the gamble is risky), estimating LA requires controlling for risk attitude (RA) through gain-only gambles involving choices between a certain gain outcome and 50% chances of a larger gain or 0 (Sokol-Hessner et al. 2013). Then, fitting simultaneously data from both trial types allows separating the contribution of LA and RA (ρ) on choices.

Although originally interpreted through a cognitive “value” function mapping objective outcomes to subjective values (Kahneman and Tversky 1979), neuroimaging evidence has shown that LA reflects a “neural loss aversion” (NLA) pattern in structures showing asymmetric activation vs. deactivation responses to prospective gains and losses, with this asymmetry tracking individual LA differences (Canessa et al. 2013; Tom et al. 2007; see Molins and Serrano 2019). This pattern was found in the ventral striatum and midcingulate cortex (more deactivated by anticipated losses than activated by gains; Canessa et al. 2013; Charpentier et al. 2016; Tom et al. 2007), and in the amygdala and posterior insula (more activated by losses than deactivated by gains; Canessa et al. 2013; Charpentier et al. 2016; Rick 2011). The insula, in particular, may mediate interoceptive modulations of LA. The latter was indeed associated with emotion regulation (Sokol-Hessner et al. 2013) and interoceptive (Sokol-Hessner et al. 2015) abilities, both associated with the insula (Kohn et al. 2014; Schulz 2016). Yet, the role of insula in LA remains debated.

On one hand, the involvement of the posterior insula in loss-avoidance learning (Samanez-Larkin et al. 2008) and avoidance behaviors (Aupperle et al. 2015; Pessiglione and Delgado 2015) supports a link between its activation and LA both during online decision-making (Canessa et al. 2013; Krawczyk and D’Esposito 2013; Schulreich et al. 2020; Tanaka et al. 2014) and at rest (Canessa et al. 2017). Moreover, LA was found positively correlated with gray matter (GM) volume in the posterior insula (Canessa et al. 2013; Li et al. 2020). However, a negative correlation was also reported between LA and GM volume in the bilateral posterior insula, possibly reflecting an anomalous detection of the salience of losses (Markett et al. 2016). Additionally, the anterior insula was found bilaterally activated when anticipating both losses and gains (Pinger et al. 2022), suggesting a generic

role in processing the salience of prospective outcomes regardless of valence. Finally, the modulation of LA by high-definition transcranial direct current stimulation (HD-tDCS) of the dorsal anterior cingulate cortex (dACC; Mattavelli et al. 2022) was not replicated with the right posterior insula (Gorrino et al. 2023). These findings challenge the view of LA as strongly linked with functional and neurostructural properties of the insula.

Several factors may explain these inconsistencies. First, the functional role of insula might vary along rostro-caudal, dorso-ventral, and hemispheric gradients (Craig 2009a, 2009b, 2015; Droutman et al. 2015). In terms of neurostructural evidence, inconsistencies may arise from techniques unveiling different features, such as voxel-based- or surface-based-morphometry (VBM/SuMB; Dias et al. 2022; Singh 2023), through univariate or multivariate approaches such as VBM/SuBM or source-based-morphometry (SoBM; Gupta et al. 2019), respectively (e.g., Markett et al. 2016; Canessa et al. 2013). Finally, measuring LA might be biased by methodological variations involving tasks (e.g., controlling for RA with gain-only trials; Tom et al. 2007; Sokol-Hessner et al. 2015), stimuli (e.g., large vs. small outcome range, or symmetric vs. asymmetric gain-loss matrices; Tom et al. 2007; De Martino et al. 2010), analytic approach (e.g., logistic regression vs. behavioral modeling; Tom et al. 2007; Sokol-Hessner et al. 2015), and neural modeling of LA. Concerning the latter aspect, while most studies assessed a linear correlation between LA and functional or structural metrics (Canessa et al. 2013; Li et al. 2020; Markett et al. 2016), there is evidence of quadratic relationships (positive “U-shaped” vs. negative “inverted U-shaped”) between cognitive-behavioral variables and brain activity/structure (Hatton et al. 2012; Mattavelli et al. 2012; Preuschhoff et al. 2006). Investigating quadratic relationships may both unveil novel properties of choice-related evaluation systems, and clarify previous conflicting reports of both positive (Canessa et al. 2013) and negative (Markett et al. 2016) correlations between LA and insular GM volume.

On these grounds, we coupled a well-established behavioral modeling approach and a comprehensive morphometric protocol to investigate both linear and quadratic relationships between LA and different voxel-based and surface-based cortical features in over 200 healthy young individuals. Based on prior findings on the neural basis of LA (Canessa et al. 2013, 2017) and insular functional organization (Craig 2009a; Droutman et al. 2015), we expected an association to engage its posterior sector, possibly in conjunction with other somatosensory nodes of the interoceptive network.

2 | Materials and Methods

See Supporting Informations for a full description of materials and methods.

2.1 | Participants

The experimental sample included 208 healthy volunteers (mean age = 24.83 years, SD = 5.71, range = 18–40; 128 females) with no history of psychiatric or neurological disorders, nor of

drug/substance use or gambling, and no current use of any psychoactive medications. They gave their written informed consent to the experimental procedure, previously approved by ICS Maugeri Ethics Committee.

2.2 | Behavioral Data Collection

We used a series of mixed-gambles to measure participants' degree of LA, under the assumption that the latter must be isolated from risk attitude (i.e., sensitivity to outcome variance) because both are involved in anticipatory evaluation processes (Sokol-Hessner et al. 2013, 2015). Before the magnetic resonance imaging (MRI) session, participants played two tasks in counter-balanced order with random shuffling of trial order. Forty-nine gain-loss gambles required to choose between the status quo (0) and a gamble that might result in equally probable (50% probability) gain or loss. The gain-loss values, sampled from a 7×7 matrix, were centered to a λ level of 2, which is representative of the general population (Brown et al. 2024; Kahneman and Tversky 1979; Ruggeri et al. 2020). Other 30 "gain-only" gambles required to choose between a certain (100% probability) gain and equal (50%) chances of a larger gain or 0.

Prior to participation, they were provided with a monetary incentive and asked to place it in their wallet (Arioli et al. 2023; Sokol-Hessner et al. 2009, 2013). They were then informed that their final payoff would depend on the outcome of one gain-loss trial and one gain-only trial randomly drawn from those played.

2.3 | MRI Data Acquisition

We used a General Electric 3 Tesla scanner (MR750 Discovery, GE Healthcare, Milwaukee, WI) to obtain a T1-weighted structural image through a 16-channel head coil and a 3D inversion-recovery-prepared fast spoiled gradient recalled (IR-FSPGR-BRAVO) sequence with 152 contiguous (in-plane resolution = 0.9375×0.9375 mm; thickness = 1 mm).

2.4 | LA Estimation

In keeping with models derived from Prospect Theory (Kahneman and Tversky 1979), the probability of accepting a gamble can be estimated as follows:

$$\Pr(\text{accept gamble} | G, L, B) = \frac{1}{1 + e^{-\mu \times (p_G \times (G)^{\rho} - \lambda \times p_L \times (-L)^{\rho} - B^{\rho})}}$$

where G is the gain, L is the loss, B is the guaranteed gain, $p_G = 0.5$ is the probability of a gain, and $p_L = 1 - p_G = 0.5$ is the probability of a loss. The free parameters of the model are: (a) LA lambda (λ), that is, the multiplicative weight associated with anticipated losses compared with gains; (b) RA rho (ρ), that is, the curvature of the value function $u(x) = x^{\rho}$ that embodies the diminishing sensitivity to increasing outcome; and (c) choice consistency or "softmax temperature" (μ), that is, a measure of noisiness vs. systematicity in choices. These parameters were

individually computed via maximum likelihood estimation with MATLAB (MathWorks, Natick, MA).

2.5 | Univariate Morphometry With Voxel-Based-Morphometry (VBM) and Surface-Based-Morphometry (SuBM)

2.5.1 | Pre-Processing of VBM and SuBM Data

T1-weighted images were first visually inspected to ensure the absence of motion artifacts and gross anatomical abnormalities potentially interfering with subsequent processing stages, which were performed with the CAT12 toolbox v.12.9/R2577 (www.neuro.uni-jena.de/cat/) and SPM12 v.7771 (<http://www.fil.ion.ucl.ac.uk/spm>).

The VBM-CAT12 pre-processing pipeline included well-established stages for: (a) correction for bias-field inhomogeneities; (b) spatial normalization with the optimized Shooting algorithm (Ashburner and Friston 2011); (c) segmentation into GM, white matter (WM) and cerebrospinal fluid (CSF) (Ashburner and Friston 2005); (d) quality control; (e) "modulation," to preserve actual GM values locally and perform volumetric analyses on "modulated" GM volumes; (f) spatially smoothing with a 8 mm isotropic Gaussian FWHM kernel. Subsequent statistical analyses were performed both on modulated and non-modulated GM images, thus providing evidence on GM absolute volume or GM density (per unit volume in native space), respectively (Smith et al. 2007).

The CAT12 pipeline for SuBM pre-processing included: (a) tissue segmentation to estimate white matter distance, and a projection-based thickness estimation jointly calculating *cortical thickness* and the central surface (Dahnke et al. 2013); (b) topological correction, through an approach based on spherical harmonics (Yotter, Dahnke, et al. 2011); (c) surface reparameterization into a common coordinate system to allow inter-subject analysis (Yotter, Thompson, and Gaser 2011); (d) spherical registration, through an adapted two-dimensional diffeomorphic DARTEL algorithm (Ashburner 2007; Yotter, Ziegler, et al. 2011); (e) extraction of the following surface types in addition to thickness: (1) *gyrification*, tracking cortical complexity in terms of folding (Luders et al. 2006); (2) *fractal dimension*, tracking local cortical complexity in terms of recursive cortical patterns (Yotter et al. 2011); (3) *sulcus depth*, based on the Euclidean distance between the central surface and its convex hull (Gaser et al. 2024); (f) surface resampling and smoothing with a Gaussian kernel of 15 mm (FWHM) for cortical thickness maps, and 20 mm (FWHM) for the other surface types.

2.5.2 | Whole-Brain Statistical Analysis of VBM and SuBM Data

Statistical analyses assessed a relationship between both the linear and quadratic components of the individual LA parameter and either regional VBM (GM volume or density) or SuBM (thickness/gyrification/fractal dimension/sulcal depth) feature metrics, while controlling for the potential effect of RA.

We used the CAT12 “cat_stat_polynomial” function, with polynomial order=2, to estimate the linear and quadratic components of the individual LA and RA parameters. For each of the aforementioned brain features, a multiple regression model tested for a relationship with both the linear and quadratic components of the LA and RA parameters. Three ancillary “control” analyses were performed. First, we replicated all analyses by modeling sex as a covariate to (a) ensure that results would be confirmed despite its association with the LA degree; (b) assess an effect of sex on the LA–brain relationship (interaction analysis). Moreover, following Sokol-Hessner et al. (2015) we computed LA as its natural logarithm, and replicated all the analyses by modeling its linear and quadratic components.

To correct for different brain sizes in terms of total intracranial volume (TIV), we analyzed modulated VBM data through an ANCOVA, after ensuring the lack of a significant correlation between TIV and the LA or RA parameters. To prevent voxel misclassification on the GM-WM border, the absolute GM threshold was set at 0.05 in VBM analyses. The resulting statistical maps were thresholded at $p < 0.05$, corrected at the cluster level with topological false discovery rate (FDR) (Chumbley et al. 2010) (forming threshold = 0.005).

We used the SPM Anatomy Toolbox (v.2.2c) (Eickhoff et al. 2005) to localize the significant clusters in the MNI space.

2.5.3 | Assessment of Robustness and Internal Consistency

To assess the internal consistency and robustness of the U-shaped relationship between behavioral LA and the reported neurostructural metrics (see Section 3.2.1), we carried out (1) a split-half analysis with Spearman-Brown correction, using 10,000 random splits of the dataset ($n = 208$) into two halves ($n = 104$ each) to estimate internal consistency, and (2) permutation testing (with 10,000 permutations) to evaluate the likelihood that the observed correlation could arise by chance (see Supporting Information).

2.5.4 | Region-of-Interest (ROI)-Based Pre-Processing and Statistical Analysis of VBM and SuBM Data

We additionally performed a ROI analysis to assess the relationship between LA and the aforementioned features in brain structures previously mapped in volume- and surface-based atlases. We extracted individual mean values of (a) GM volume (in mL) from the “Anatomy v.3” (Eickhoff et al. 2005) and “Local-Global Intrinsic Functional Connectivity Parcellation” (600 parcels; Schaefer et al. 2018) atlases, and (b) the aforementioned surface features from the Aparc2009 (Destrieux et al. 2010) atlas. For all features, we performed correlation analyses between individual tissue volumes and both the linear and quadratic components of the LA parameter, using Pearson’s r coefficient and a statistical threshold of $p < 0.05$ FDR corrected for multiple comparisons.

2.6 | Multivariate Morphometry With SoBM

2.6.1 | SoBM (Pre)processing

SoBM employs spatial independent component analysis (ICA) to decompose GM images into maximally independent spatial sources, that is, independent patterns in GM images representing “natural structural networks” (Xu et al. 2009). The expression of such patterns in single subjects is quantified by a “loading coefficient” that can be modeled in statistical analyses to investigate its relationship with variables of interest and/or group differences. After image pre-processing, SoBM therefore entails ICA and statistical analysis. We thus performed spatial ICA on the same modulated GM images that also entered VBM analyses, using the GIFT toolbox (<http://icatb.sourceforge.net>; Calhoun et al. 2001) to perform ICA through the Infomax neural network algorithm (Bell and Sejnowski 1995). ICA was repeated 250 times in Icasso (<http://research.ics.aalto.fi/ica/icasso/>), and the resulting components were clustered to ensure the reliability of the results, which are quantified using a quality index (Iq) ranging from 0 to 1 and reflecting the difference between intra-cluster and extra-cluster similarity (Himberg et al. 2004). We extracted 31 independent components (ICs) from the GM images, all associated with an Iq > 0.8 indicating a highly stable ICA decomposition (Allen et al. 2011), that were anatomically labeled with the Anatomy-Toolbox (v2.2c) (Eickhoff et al. 2005).

2.6.2 | SoBM Statistical Analysis

For all the extracted components we performed correlation analyses between individual loading coefficients and both the linear and quadratic components of the LA parameter, with a statistical threshold of $p < 0.05$ FDR-corrected. For each of the components showing a significant relationship between the loading coefficient and LA, we additionally used a “Homogeneity of slopes” test to assess whether that effect was significantly different across (a) the linear and quadratic components; (b) female and male participants.

3 | Results

3.1 | Behavioral Results

In keeping with a well-established literature (Brown et al. 2024), the mean and median of behavioral LA were 2.088 and 1.944 (SD = 0.816), respectively, with slightly but significantly higher values in females (mean LA = 2.190, SD = 0.910) than males (mean LA = 1.924, SD = 0.608) ($t(206) = 2.317$, $p = 0.021$). The mean LA degree of our sample was significantly higher than the “loss-indifference” $\lambda = 1$ ($t(207) = 19.224$, $p < 0.0001$) but not significantly different from $\lambda = 2$ ($t(207) = 1.559$, $p = 0.120$), which confirms the tendency to weigh potential losses about twice as much as potential gains in decision-making under risk.

3.2 | VBM and SuBM Results

3.2.1 | Whole-Brain VBM and SuBM Results

A positive correlation with the quadratic component of LA (reflecting a U-shaped relationship) was found with GM volume in two clusters encompassing bilaterally the posterior insular cortex and parietal operculum (OP1 and OP4), as well as inferior parietal and sensorimotor cortex (areas 1, 2, and 3b) (Table 1 and Figure 1). A U-shaped relationship with GM density was found in the left posterior insula and rolandic/parietal operculum (OP1 and OP3), as well as in a cluster encompassing the ventral

striatum and thalamus (Table 1 and Figure 1). No significant correlation was found for the linear component of LA.

Concerning surface features, LA was linearly negatively correlated with the degree of gyrification in the left middle frontal gyrus (Table 1 and Figure 1). Moreover, there was a U-shaped relationship between LA and gyrification in the medial orbitofrontal cortex. No significant relationship was found for the other surface metrics (Table 1 and Figure 1).

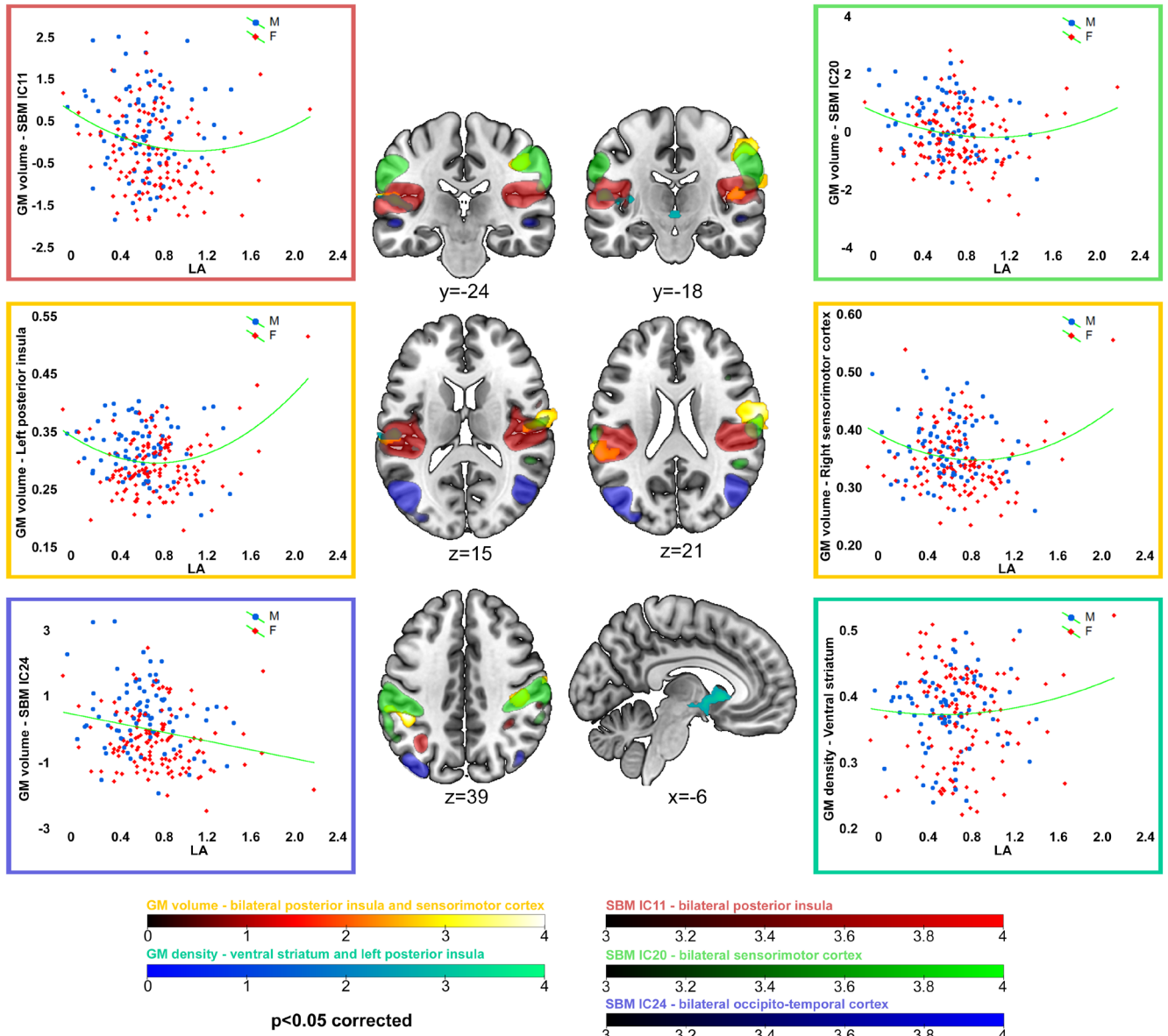
These findings were confirmed when modeling sex as covariate of no interest (Table S1). Supporting this finding, interaction

TABLE 1 | Whole-brain results from univariate voxel-based-morphometry and surface-based-morphometry.

K	H	Anatomical region	Cytoarchitectonic mapping	x	y	z	T-score
“U-shaped” correlation with GM volume							
3466	R	Postcentral gyrus		64	−3	27	4.49
		Postcentral gyrus	3b	62	−9	18	3.96
		Precentral gyrus	1	51	−18	46	3.37
		Posterior insular cortex	OP1 [SII]	48	−18	10	3.35
		Parietal operculum	OP4 [PV]	64	2	4	3.22
		Supramarginal gyrus		70	−20	18	2.94
2591	L	Inferior parietal lobule	hIP2 (IPS)	−46	−39	40	4.65
		Supramarginal gyrus	PFt (IPL)	−57	−33	36	3.83
		Supramarginal gyrus	PF (IPL)	−62	−39	24	3.75
		Parietal operculum	OP1 [SII]	−54	−24	14	3.4
		Parietal operculum	OP1 [SII]	−62	−26	15	3.21
		Postcentral gyrus	2	−34	−40	62	3.15
		Rolandic operculum	PFcm (IPL)	−40	−34	18	2.66
“U-shaped” correlation with GM density							
1354	L/R	Ventral striatum		−2	15	2	3.81
		Ventral striatum		3	2	−15	3.4
		Thalamus		−3	−4	−8	3.15
		Thalamus		3	−18	−6	2.78
1351	L	Superior temporal gyrus		−56	−20	9	3.84
		Parietal operculum	OP1 [SII]	−52	−22	10	3.78
		Insula lobe	Ig2	−42	−14	4	3.34
		Insula lobe	OP3 [VS]	−38	−10	8	3.22
		Rolandic operculum		−39	−33	15	2.81
Negative linear correlation with gyrification							
1284	L	Middle frontal gyrus		−29	37	22	3.92
“U-shaped” correlation with gyrification							
3	R	Orbitofrontal cortex	Fo1	13	27	−17	5.98

Note: From left to right, the table reports the extent (K, in number of $1.5 \times 1.5 \times 1.5 \text{ mm}^3$ voxels), hemispheric lateralization, anatomical labeling based on the Anatomy Toolbox (v2.2c; Eickhoff et al. 2005), stereotactic coordinates and statistical-value of the correlation between the linear or quadratic components of behavioral LA and (a) GM volume or GM density from VBM analyses, or (b) degree of gyrification (i.e., cortical complexity from SuBM analyses). Abbreviations: Fo1: medial orbitofrontal cortex; hIP: human Intraparietal; Ig: granular posterior insular lobe; OP: parietal operculum.

Voxel-Based-Morphometry and Source-Based-Morphometry



Surface-Based-Morphometry

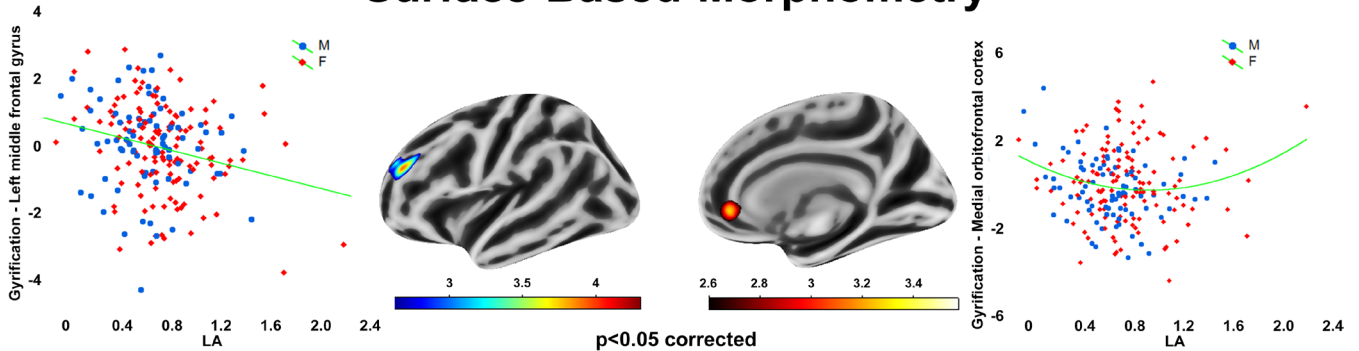


FIGURE 1 | Morphometric results. The top figure sector depicts the brain structures showing a significant relationship with the linear or quadratic components of behavioral LA (as shown by the respective scatterplots), that is, GM volume in the posterior insular cortex (VBM: yellow-orange; SBM-IC11: red), sensorimotor cortex (VBM: yellow-orange; SBM-IC20: green), and occipito-temporal cortex (SBM-IC24: blue), as well as GM density in the ventral striatum and posterior insula (VBM: cyan). The bottom sector depicts the left middle frontal gyrus (left) and medial orbitofrontal cortex (right) in which cortical complexity (gyrfication) shows, respectively, a negative linear and a U-shaped relationship with LA.

analyses highlighted no significant effect of sex on the LA–GM relationship. Moreover, modeling the linear or quadratic components of the logarithm of LA only resulted in a U-shaped relationship with GM volume in the left inferior parietal cortex (hIP2; $\chi^2 = -46-39\ 38$; FWE-corrected $p = 0.029$).

Split-half analyses yielded Spearman–Brown reliability coefficients ranging from 0.3 to 0.4 for all the clusters showing a whole-brain significant U-shaped relationship between LA and GM volume or density, and a coefficient of 0.279 for OFC gyrification (Table S2). While falling within a range of limited internal consistency, these values fit with the average reliability levels typically reported for brain-behavior associations in task-based fMRI studies (e.g., 0.228–0.397 in Elliott et al. 2020). Moreover, permutation testing revealed statistically significant correlations ranging from 0.284 to 0.348 for GM volume or density, and a correlation index of 0.207 for OFC gyrification (Table S2), confirming the robustness of relationships that are unlikely due to random associations.

3.2.2 | ROI-Based VBM and SuBM Results

ROI analyses confirmed a U-shaped relationship between LA and GM volume in the right parietal operculum (OP4, $r = 0.244$, FDR-corrected $p = 0.041$) and left inferior parietal cortex (PFcm, $r = 0.241$, FDR-corrected $p = 0.041$) of the Anatomy v.3 atlas, and with GM volume of the right sensorimotor cortex (SomMotA_1, $r = 0.254$, FDR-corrected $p = 0.048$; SomMotB_Cent_1, $r = 0.262$, FDR-corrected $p = 0.048$; rSomMotB_S2_8, $r = 0.252$, FDR-corrected $p = 0.048$) of the Schaefer 600 atlas. Instead, there was no significant relationship between GM volume and the linear component of LA, nor between GM density and any LA metric.

As to surface metrics, ROI analyses confirmed a linear negative correlation between LA and the degree of gyrification in the left middle frontal cortex (IS_front_middle, $r = -0.257$, FDR-corrected $p = 0.026$). Moreover, there was evidence of a quadratic relationship between LA and fractal dimension in three clusters. This relationship was positive (i.e., U-shaped) in the left short posterior insular gyrus (IG_insular_short, $r = 0.242$, FDR-corrected $p = 0.029$) and negative (i.e., inverted U-shaped) both in the left frontomarginal sulcus and gyrus (IG_and_S_frontomargin, $r = -0.236$, FDR-corrected $p = 0.029$) in the lateral orbitofrontal cortex and in the right posterior transverse collateral sulcus (rS_collat_transv_post, $r = -0.246$, FDR-corrected $p = 0.029$) in the medial occipito-temporal cortex.

Also for ROI analyses, there was no significant interactive effect of sex on the relationship between LA and cortical features.

3.3 | SoBM Results

We extracted 31 reliable ICs from GM-volume images, representing naturally grouped voxels showing similar covariation among subjects (i.e., “natural structural networks”; Gupta et al. 2019; Xu et al. 2009) still with differential inter-individual expression as captured by their loading coefficient. Correlation analyses showed that LA was linearly negatively correlated

with the loading coefficient of IC24 ($r = -0.194$, FDR- $p = 0.011$), including distinct clusters in the left occipito-temporal cortex and in the right inferior, middle and superior temporal cortex (Table 2 and Figure 1). Instead, there was a U-shaped relationship with both IC11 ($r = 0.188$, FDR- $p = 0.007$), involving the posterior insular cortex, parietal operculum and inferior parietal cortex bilaterally, and IC20 ($r = 0.218$, FDR- $p = 0.002$), encompassing the postcentral gyrus and inferior parietal cortex bilaterally, plus the left inferior-middle temporal cortex (Table 2 and Figure 1).

Such relationship was significantly stronger with the linear than the quadratic component for IC24 ($r(\text{linear}) = -0.194$, $p = 0.002$; $r(\text{quadratic}) = 0.043$, $p = 0.529$; $F(1) = 9.467$, $p = 0.002$), while the opposite was true for IC11 ($r(\text{linear}) = -0.086$, $p = 0.216$; $r(\text{quadratic}) = 0.188$, $p = 0.013$; $F(1) = 4.332$, $p = 0.038$), with a marginal evidence for IC20 ($r(\text{linear}) = -0.050$, $p = 0.470$; $r(\text{quadratic}) = 0.218$, $p = 0.002$; $F(1) = 3.439$, $p = 0.064$). Instead, for none of these components the relationship with LA was significantly different across female and male participants.

4 | Discussion

Recent advances in neuroeconomics have shown that individual differences in decision-making are also influenced by interoceptive sensitivity (Herman et al. 2021; Sokol-Hessner et al. 2015) and its insular-somatosensory neural correlates (Pleger and Villringer 2013; Poppa and Bechara 2018; Romo et al. 2012). However, the insula’s role in LA remains debated, with studies reporting both positive (Canessa et al. 2013) and negative (Markett et al. 2016) correlations between their structural properties. To fill this gap, we used a comprehensive morphometric approach to investigate both the linear and quadratic relationships between LA and different voxel-based (GM volume and density) and surface-based (thickness/gyrification/fractal dimension/sulcal depth) cortical features in 208 healthy young participants. Multivariate analyses with source-based morphometry allowed for grounding such relationships in “structural networks” spanning anatomically distinct regions (Caprihan et al. 2011). As predicted, we identified significant associations between LA and cortical features within two structural networks encompassing the posterior portion of the peri-insular sulcus (posterior insula alongside parietal and temporal opercula) and somatosensory-parietal areas (supramarginal gyrus [SMG] and sensorimotor cortex). These data support the hypothesis that individual differences in LA are also shaped by interoceptive drives involving the posterior insula (Craig 2009a; Gu and FitzGerald 2014), and provide novel evidence helping explain previous controversial results on this topic.

The key finding is that both univariate and multivariate analyses highlighted a U-shaped association between LA and cortical features of posterior insular and somatosensory-parietal areas (Figure 1). Namely, the largest values across most structural features were observed in the individuals with the highest and lowest LA levels. This evidence aligns with the notion of the posterior insula as a key hub for detecting salient stimuli and representing body-state responses to salient stimuli (Menon and Uddin 2010), with the latter also involving somatosensory areas processing somatic sensory information (Hegarty et al. 2020;

TABLE 2 | Results from multivariate source-based-morphometry.

K	H	Anatomical region	Cytoarchitectonic mapping	x	y	z	T-score
IC11: “U-shaped” correlation with GM volume							
6754	L	Superior temporal gyrus		-42	-34	15	9.53
		supramarginal gyrus	PFcm (IPL)	-51	-39	24	8.66
		Superior temporal gyrus		-54	-21	6	7.36
		Rolandic operculum		-40	-6	12	3.41
5889	R	Rolandic operculum	OP1 [SII]	42	-28	18	10.24
		Superior temporal gyrus		58	-10	4	5.56
		Rolandic operculum	OP4 [PV]	56	-4	6	5.28
742	L	Angular gyrus	hIP3 (IPS)	-34	-62	40	8.45
262	R	Inferior parietal lobule	hIP3 (IPS)	36	-45	42	4.26
IC20: “U-shaped” correlation with GM volume							
6771	R	Postcentral gyrus	2	48	-24	42	10.19
		Supramarginal gyrus	1	60	-16	28	9.59
		Middle temporal gyrus		52	-40	9	4.12
		Supramarginal gyrus	PFm (IPL)	54	-44	34	3.78
6716	L	Inferior parietal lobule	PFt (IPL)	-48	-30	40	10.11
		Angular gyrus	PGa (IPL)	-51	-57	30	4.15
303	L	Inferior temporal gyrus		-60	-54	-6	3.8
		Middle temporal gyrus		-64	-46	-8	3.5
IC24: Negative linear correlation with GM volume							
8257	L	Middle temporal gyrus		-44	-70	18	11.9
		Middle occipital gyrus	PGp (IPL)	-42	-76	34	7.2
		Middle occipital gyrus	hOc4la	-46	-72	2	6.37
		Inferior temporal gyrus		-45	-64	-6	6.3
		Middle occipital gyrus	hOc4lp	-33	-88	20	4.34
3846	R	Middle temporal gyrus		45	-69	18	9.89
692	R	Inferior temporal gyrus		48	-38	-22	4.82
		Inferior temporal gyrus	FG4	44	-56	-14	4.74
		Fusiform gyrus	FG4	45	-45	-16	4.62

Note: From left to right, the table reports the extent (K, in number of $1.5 \times 1.5 \times 1.5 \text{ mm}^3$ voxels), hemispheric lateralization, anatomical labeling based on the Anatomy Toolbox (v2.2c; Eickhoff et al. 2005), stereotactic coordinates and statistical-value of the correlation between the linear or quadratic components of behavioral LA and the loading coefficient of the structural networks (i.e., independent components) resulting from SoBM analyses on GM volume segmentations. Abbreviations: FG: fusiform gyrus; hIP: human intraparietal; hOc4: lateral occipital cortex; OP: parietal operculum.

Jalon et al. 2023). This pattern fits with prior reports of U-shaped responses to the extreme values of different types of salient stimuli, such as perceived intelligence (most unintelligent and most intelligent-looking faces; Akimoto et al. 2018) or similarity to a danger-cue (most similar and most unsimilar stimuli; Webler et al. 2021) for the insula, laugh authenticity (Lavan et al. 2017) for the SMG, and emotional valence of voices (highly negative and highly positive stimuli; Bestelmeyer et al. 2017) for both structures. This evidence consistently suggests that the insula is sensitive to the *salience* of stimuli more than their valence,

which in turn helps interpret its involvement in the interoceptive modulation of LA (Sokol-Hessner et al. 2015).

The previously reported bilateral activation of the insula to the anticipation of both losses and gains (Pinger et al. 2022) suggests that the stronger sensitivity to salience than valence holds for economic prospects, thus likely representing a transversal interoceptive reactivity to behaviorally relevant stimuli. Without questioning the well-known asymmetry between loss-avoidant and reward-seeking drives inherent in the

notion of LA (Sokol-Hessner and Rutledge 2019), a prominent sensitivity of the insular and somatosensory-parietal cortex to the largest gain *and* loss values (Haufler et al. 2022; Pinger et al. 2022) might explain its association with opposite behavioral drives. These structures might drive both loss-avoidant behavior (high LA) when facing potential losses that are sensed as excessively large (or not sufficiently small) compared with prospective gains, and reward-seeking behavior (low LA) when potential gains are valued as sufficiently large to be worth the risk (Hu et al. 2024). The same valence-free salience detection mechanism might thus explain the present evidence of a two-sided relationship between LA and both insular and somatosensory-parietal GM volume (Figure 1). This perspective, which emphasizes sensitivity to high- versus low-salience outcomes rather than negative versus positive outcomes, may help explain why everyday decision-making is shaped by contextual cues that define outcome salience (Kutlu et al. 2021). The U-shaped relationship between LA and posterior insular GM volume suggests that effective decision-making depends on balanced, rather than blunted or heightened, engagement of emotional and bodily signals. Such balance may promote uncertainty tolerance and behavioral flexibility, supporting more adaptive, context-sensitive risk assessments aligned with situational demands.

A U-shaped relationship with LA was identified, in the left posterior insula, also for GM density and fractal dimension. The latter indexes cortical complexity in terms of recursive patterns in cortical surfaces (Yotter et al. 2011; Meregalli et al. 2022), and has been previously associated with cognitive efficiency in healthy young adults (Im et al. 2006), and with cognitive decline in healthy aging (McDonough and Madan 2021; Mustafa et al. 2012) and neurodegenerative disorders (Nicastro et al. 2020). These findings complement previous preliminary results on the hemispheric lateralization of interoceptive and affective processes (Craig 2009a, 2009b). Our data support a left-hemispheric contribution consistent with previous findings on both LA (Li et al. 2020; Markett et al. 2016) and emotional processing (Duerden et al. 2013) in healthy individuals, and with clinical reports of altered emotional processing following left posterior insular damage (Borg et al. 2013). Notably, also sex may influence the lateralization of insular involvement in emotional processing, with females and males recruiting preferentially the left and right posterior insula, respectively (Duerden et al. 2013). The lack of sex effects in our morphometric data, despite significant behavioral differences, suggests that a different hemispheric association with LA between females and males might mainly involve the functional, rather than structural, level.

Observing a U-shaped relationship between LA and posterior insular features helps clarify previous inconsistent evidence of both positive (Canessa et al. 2013) and negative (Markett et al. 2016) correlations with GM volume in this region. A U-shaped relationship might indeed result in opposite findings if inherent features of the stimuli, or their calibration to participant's LA level, favor either the descending or ascending parts of the curve for low and high LA levels, respectively. Consistently with this hypothesis, positive and negative correlations between LA and insular GM volume have been found using, respectively, a symmetric gain-loss matrix (Canessa et al. 2013) versus a smaller range of potential losses (Markett et al. 2016). As suggested by the author

themselves, in the latter study a relatively small loss range—generating more positive expected values—might have biased sampling toward lower LA values (Markett et al. 2016), thus favoring the descending part of a U-shaped curve.

This interpretation also applies to the U-shaped relationship between LA and GM density in the ventral striatum and thalamus. Although typically associated with reward-seeking behavior (Grill et al. 2021), the striatum is indeed a key node of a “neural LA” network showing a greater deactivation for anticipated losses than activation for gains that correlate with the individual LA level (Canessa et al. 2013; Charpentier et al. 2016; Tom et al. 2007; see Molins and Serrano 2019). Also in the striatum, the presence of both gain- and loss-related responses may support positive *and* negative correlations with LA, depending on multiple factors facilitating the detection of the descending part of a U-shaped curve (a negative relationship consistent with the striatum role in reward-seeking; Jauhar et al. 2021), or of the ascending one (underpinning the striatal contribution to loss avoidance alongside posterior insula and thalamus). The latter is indeed considered to enhance aversive motivational drives by relaying viscerosensory and nociceptive information that informs the posterior insula about bodily states (Craig 2002; Critchley et al. 2002; Ploghaus et al. 1999), thus promoting avoidance behaviors that are additionally reinforced by the coding of aversive prediction errors in the ventral striatum (Thiele et al. 2021). While these findings support the view that posterior insula, striatum, and thalamus collectively contribute to shape LA, observing a quadratic relationship between their metrics suggests that this modulation is more complex than a mere facilitation of avoidant behavior (Charpentier et al. 2016; LeDoux 2012; Schlund et al. 2010).

Concerning surface-based data, a quadratic relationship with LA was also found for fractal dimension and gyrification. The latter is a further metric of cortical complexity, tracking the degree of folding (Luders et al. 2006), that was found associated with cognitive performance (Gregory et al. 2016) and with neurocognitive decline both in normal aging (Lamballais et al. 2020) and neurological conditions (Xiao et al. 2024). In particular, we observed opposite associations between LA and cortical complexity in the medial OFC (U-shaped correlation with gyrification in whole-brain analysis) and lateral OFC (inverted U-shape correlation with fractal dimension in ROI analyses). Like the ventral striatum, the medial OFC is a key node of the “neural LA” network (Tom et al. 2007), displaying both gain- and loss-related responses that might explain the presence of both negative and positive correlations at the extremes of the quadratic relationship with LA. The inversion of such relationship in the medial versus lateral OFC supports previous proposals on their opposite functional roles (Rolls 2019; Rolls et al. 2020) in processing positive vs. negative choice-related stimuli, respectively (Groman et al. 2019). Their responsiveness to positive and negative outcomes however depends on the decision-making context, to the point of reversing the associated affective reactions when a same outcome is compared with an alternative counterfactual, rather than an actual, outcome (Canessa et al. 2009, 2011; Ursu and Carter 2005). In this complex pattern, the medial OFC might enhance the salience of both gains and losses, thus favoring the extreme LA levels associated with maximum loss avoidance or reward seeking. Conversely, the role played

by the lateral OFC in anticipating negative feelings associated both with potential losses and missed rewards might explain its association with medium LA levels. This interpretation fits with the OFC role in reversal-learning and behavioral flexibility (Rudebeck and Rich 2018), although further evidence is needed to unveil the complex relationship between cortical features and cognitive-behavioral parameters.

This consideration raises questions and limitations about the functional meaning of the observed correlations (Mechelli et al. 2005). Cortical features such as GM volume and density are differentially shaped by distinct histological factors, including neuronal and glial density, dendritic arborization, number of axonal projections, and extent of myelination (Gennatas et al. 2017). These properties influence “input” connections, in turn shaping communication with downstream network nodes (Pareek et al. 2018; Vignando et al. 2019). Moreover, although the application of corrected statistical thresholds and control analyses via permutation testing ensured robust findings, the observed associations between neurostructural metrics and LA were generally weak. This is not surprising, as other explanatory levels such as structural and functional connectivity might be expected to shape LA even more than GM features. This consideration may account for the limited internal consistency observed in the present findings, which nonetheless aligns with the levels typically reported for brain-behavior associations in task-based fMRI studies (Elliott et al. 2020). All these limitations point to the importance of addressing this relationship with a multimodal approach merging distinct (f)MRI features.

Notwithstanding these limitations, we showed that the relationship between LA and cortical features mostly follows a quadratic, U-shaped, trend. We observed only one linear relationship, that is, a negative correlation between LA and gyrification in the left dorsolateral prefrontal cortex highlighted both by whole-brain and ROI analyses. This region is known to underpin the interface between decision-making and action selection (Dixon and Christoff 2014; Zha et al. 2019), and its activity was previously found to correlate positively with potential gains and negatively with losses (e.g., Xu et al. 2020), which suggests a role in reward-anticipation possibly counteracting the spontaneous LA attitude.

5 | Conclusion

We showed for the first time that the relationship between LA and posterior insular and somatosensory-parietal features follows a quadratic U-shaped rather than linear trend, supporting the role of structural networks potentially mediating an interoceptive boost to LA. This pattern may help reconcile previous conflicting reports of positive (Canessa et al. 2013; Li et al. 2020) and negative (Markett et al. 2016) correlations between them, highlighting the need to investigate brain-behavior relationships at higher-order levels.

Notably, both extremely low and high LA levels—here associated with posterior insular and somatosensory features—have been linked to specific clinical conditions, including addiction (Canessa et al. 2022; Genauck et al. 2017; Gianelli et al. 2022)

and anxiety (Xu et al. 2020; but see Charpentier et al. 2016), respectively. These disorders are characterized not only by impairments in outcome anticipation and decision-making (Hartley and Phelps 2012; Koffarnus and Kaplan 2018) but also by altered emotion regulation (Cisler et al. 2010; Stellern et al. 2023) and interoceptive awareness (Clemente et al. 2024; Domschke et al. 2010; Paulus and Stewart 2014; Verdejo-Garcia et al. 2012). By implicating insular and somatosensory networks in emotional difficulties and maladaptive decision-making (Tan et al. 2022), these findings may inform clinical interventions based on neuro-psycho-physiological measures, such as neurofeedback targeting insular activity (Linhartová et al. 2019) or modulation of bodily signals including heart rate, respiration, and skin conductance (Jerčić and Sundstedt 2019) to support emotional regulation. Such approaches may facilitate the recognition of arousal responses to emotional contexts, thereby potentially enhancing interoceptive awareness, promoting effective emotion regulation strategies (e.g., cognitive reappraisal over suppression), and ultimately supporting adaptive decision-making (Ter Harmse et al. 2021; Jerčić and Sundstedt 2019).

Author Contributions

Maria Arioli: conceptualization, data curation, investigation, methodology, project administration, writing—original draft. **Giulia Mattavelli:** investigation, methodology. **Letizia Richelli:** data curation, writing – editing. **Zaira Cattaneo:** investigation, resources. **Paolo Poggi:** investigation, resources. **Nicola Canessa:** conceptualization, data curation, investigation, formal analysis, methodology, project administration, supervision, writing – original draft.

Acknowledgments

This research was partially supported by the “Ricerca Corrente” funding scheme of the Italian Ministry of Health to ICS Maugeri, and the “Dipartimenti di Eccellenza 2023–2027” funding scheme of the Italian Ministry of University and Research to IUSS Pavia. The funding source had no role in any stage of the project. Open access funding provided by BIBLIOSAN.

Conflicts of Interest

The authors declare no conflicts of interest.

Data Availability Statement

The data that support the findings of this study are available from the corresponding author upon reasonable request.

References

- Akimoto, Y., R. Yamazaki, M. Sugiura, et al. 2018. “Approach or Avoidance: Neural Correlates of Intelligence Evaluation From Faces.” *European Journal of Neuroscience* 48, no. 1: 1680–1690. <https://doi.org/10.1111/ejn.13974>.
- Allen, E. A., E. B. Erhardt, E. Damaraju, et al. 2011. “A Baseline for the Multivariate Comparison of Resting-State Networks.” *Frontiers in Systems Neuroscience*, ahead of print, February 04. <https://doi.org/10.3389/fnsys.2011.00002>.
- Arioli, M., G. Basso, G. Baud-Bovy, L. Mattioni, P. Poggi, and N. Canessa. 2023. “Neural Bases of Loss Aversion When Choosing for Oneself Versus Known or Unknown Others.” *Cerebral Cortex* 33, no. 11: 7120–7135. <https://doi.org/10.1093/cercor/bhad025>.

- Ashburner, J. 2007. "A Fast Diffeomorphic Image Registration Algorithm." *NeuroImage* 38, no. 1: 95–113. <https://doi.org/10.1016/j.neuroimage.2007.07.007>.
- Ashburner, J., and K. J. Friston. 2005. "Unified Segmentation." *NeuroImage* 26, no. 3: 839–851. <https://doi.org/10.1016/j.neuroimage.2005.02.018>.
- Ashburner, J., and K. J. Friston. 2011. "Diffeomorphic Registration Using Geodesic Shooting and Gauss–Newton Optimisation." *NeuroImage* 55, no. 3: 954–967. <https://doi.org/10.1016/j.neuroimage.2010.12.049>.
- Aupperle, R. L., A. J. Melrose, A. Francisco, M. P. Paulus, and M. B. Stein. 2015. "Neural Substrates of Approach-Avoidance Conflict Decision-Making." *Human Brain Mapping* 36, no. 2: 449–462. <https://doi.org/10.1002/hbm.22639>.
- Bechara, A. 2000. "Emotion, Decision Making and the Orbitofrontal Cortex." *Cerebral Cortex* 10, no. 3: 295–307. <https://doi.org/10.1093/cercor/10.3.295>.
- Bell, A. J., and T. J. Sejnowski. 1995. "An Information-Maximization Approach to Blind Separation and Blind Deconvolution." *Neural Computation* 7, no. 6: 1129–1159. <https://doi.org/10.1162/neco.1995.7.6.1129>.
- Berntson, G. G., and S. S. Khalsa. 2021. "Neural Circuits of Interoception." *Trends in Neurosciences* 44, no. 1: 17–28. <https://doi.org/10.1016/j.tins.2020.09.011>.
- Bestelmeyer, P. E. G., S. A. Kotz, and P. Belin. 2017. "Effects of Emotional Valence and Arousal on the Voice Perception Network." *Social Cognitive and Affective Neuroscience* 12, no. 8: 1351–1358. <https://doi.org/10.1093/scan/nsx059>.
- Borg, C., N. Bedoin, R. Peyron, S. Bogey, B. Laurent, and C. Thomas-Antérion. 2013. "Impaired Emotional Processing in a Patient With a Left Posterior Insula-SII Lesion." *Neurocase* 19, no. 6: 592–603. <https://doi.org/10.1080/13554794.2012.713491>.
- Brown, A. L., T. Imai, F. M. Vieider, and C. F. Camerer. 2024. "Meta-Analysis of Empirical Estimates of Loss Aversion." *Journal of Economic Literature* 62, no. 2: 485–516.
- Calhoun, V. D., T. Adali, G. D. Pearlson, and J. J. Pekar. 2001. "A Method for Making Group Inferences From Functional MRI Data Using Independent Component Analysis." *Human Brain Mapping* 14, no. 3: 140–151. <https://doi.org/10.1002/hbm.1048>.
- Canessa, N., C. Crespi, G. Baud-Bovy, et al. 2017. "Neural Markers of Loss Aversion in Resting-State Brain Activity." *NeuroImage* 146: 257–265. <https://doi.org/10.1016/j.neuroimage.2016.11.050>.
- Canessa, N., C. Crespi, M. Motterlini, et al. 2013. "The Functional and Structural Neural Basis of Individual Differences in Loss Aversion." *Journal of Neuroscience* 33, no. 36: 14307–14317. <https://doi.org/10.1523/JNEUROSCI.0497-13.2013>.
- Canessa, N., G. Basso, P. Poggi, and C. Gianelli. 2022. "Altered Striatal-Opercular Intrinsic Connectivity Reflects Decreased Aversion to Losses in Alcohol Use Disorder." *Neuropsychologia* 172: 108258.
- Canessa, N., M. Motterlini, C. Di Dio, et al. 2009. "Understanding Others' Regret: A fMRI Study. Ed. Mark A. Williams." *PLoS One* 4: e7402. <https://doi.org/10.1371/journal.pone.0007402>.
- Canessa, N., M. Motterlini, F. Alemanno, D. Perani, and S. F. Cappa. 2011. "Learning From Other People's Experience: A Neuroimaging Study of Decisional Interactive-Learning." *NeuroImage* 55: 353–362. <https://doi.org/10.1016/j.neuroimage.2010.11.065>.
- Caprihan, A., C. Abbott, J. Yamamoto, et al. 2011. "Source-Based Morphometry Analysis of Group Differences in Fractional Anisotropy in Schizophrenia." *Brain Connectivity* 1, no. 2: 133–145. <https://doi.org/10.1089/brain.2011.0015>.
- Charpentier, C. J., B. D. Martino, A. L. Sim, T. Sharot, and J. P. Roiser. 2016. "Emotion-Induced Loss Aversion and Striatal-Amygdala Coupling in Low-Anxious Individuals." *Social Cognitive and Affective Neuroscience* 11, no. 4: 569–579. <https://doi.org/10.1093/scan/nsv139>.
- Chen, W. G., D. Schloesser, A. M. Arensdorf, et al. 2021. "The Emerging Science of Interoception: Sensing, Integrating, Interpreting, and Regulating Signals Within the Self." *Trends in Neurosciences* 44, no. 1: 3–16.
- Chumbley, J., K. Worsley, G. Flandin, and K. Friston. 2010. "Topological FDR for Neuroimaging." *NeuroImage* 49, no. 4: 3057–3064. <https://doi.org/10.1016/j.neuroimage.2009.10.090>.
- Cisler, J. M., B. O. Olatunji, M. T. Feldner, and J. P. Forsyth. 2010. "Emotion Regulation and the Anxiety Disorders: An Integrative Review." *Journal of Psychopathology and Behavioral Assessment* 32: 68–82.
- Clemente, R., A. Murphy, and J. Murphy. 2024. "The Relationship Between Self-Reported Interoception and Anxiety: A Systematic Review and Meta-Analysis." *Neuroscience and Biobehavioral Reviews* 167: 105923.
- Craig, A. D. (Bud). 2015. *How Do You Feel? An Interoceptive Moment with Your Neurobiological Self*. Princeton University Press.
- Craig, A. D. 2002. "How Do You Feel? Interoception: The Sense of the Physiological Condition of the Body." *Nature Reviews Neuroscience* 3, no. 8: 655–666. <https://doi.org/10.1038/nrn894>.
- Craig, A. D. 2009a. "How Do You Feel—Now? The Anterior Insula and Human Awareness." *Nature Reviews Neuroscience* 10, no. 1: 59–70. <https://doi.org/10.1038/nrn2555>.
- Craig, A. D., (Bud). 2009b. "Emotional Moments Across Time: A Possible Neural Basis for Time Perception in the Anterior Insula." *Philosophical Transactions of the Royal Society, B: Biological Sciences* 364, no. 1525: 1933–1942. <https://doi.org/10.1098/rstb.2009.0008>.
- Critchley, H. D., C. J. Mathias, and R. J. Dolan. 2002. "Fear Conditioning in Humans: The Influence of Awareness and Autonomic Arousal on Functional Neuroanatomy." *Neuron* 33, no. 4: 653–663. [https://doi.org/10.1016/S0896-6273\(02\)00588-3](https://doi.org/10.1016/S0896-6273(02)00588-3).
- Dahnke, R., R. A. Yotter, and C. Gaser. 2013. "Cortical Thickness and Central Surface Estimation." *NeuroImage* 65: 336–348. <https://doi.org/10.1016/j.neuroimage.2012.09.050>.
- De Martino, B., C. F. Camerer, and R. Adolphs. 2010. "Amygdala Damage Eliminates Monetary Loss Aversion." *Proceedings of the National Academy of Sciences of the United States of America* 107, no. 8: 3788–3792. <https://doi.org/10.1073/pnas.0910230107>.
- Destrieux, C., B. Fischl, A. Dale, and E. Halgren. 2010. "Automatic Parcellation of Human Cortical Gyri and Sulci Using Standard Anatomical Nomenclature." *NeuroImage* 53, no. 1: 1–15. <https://doi.org/10.1016/j.neuroimage.2010.06.010>.
- Dias, M. D. F. M., P. Carvalho, M. Castelo-Branco, and J. Valente Duarte. 2022. "Cortical Thickness in Brain Imaging Studies Using FreeSurfer and CAT12: A Matter of Reproducibility." *Neuroimage: Reports* 2, no. 4: 100137. <https://doi.org/10.1016/j.yrnirp.2022.100137>.
- Dixon, M. L., and K. Christoff. 2014. "The Lateral Prefrontal Cortex and Complex Value-Based Learning and Decision Making." *Neuroscience & Biobehavioral Reviews* 45: 9–18. <https://doi.org/10.1016/j.neubiorev.2014.04.011>.
- Domschke, K., S. Stevens, B. Pfeleiderer, and A. L. Gerlach. 2010. "Interoceptive Sensitivity in Anxiety and Anxiety Disorders: An Overview and Integration of Neurobiological Findings." *Clinical Psychology Review* 30, no. 1: 1–11. <https://doi.org/10.1016/j.cpr.2009.08.008>.
- Droutman, V., A. Bechara, and S. J. Read. 2015. "Roles of the Different Sub-Regions of the Insular Cortex in Various Phases of the Decision-Making Process." *Frontiers in Behavioral Neuroscience* 9: 309. <https://doi.org/10.3389/fnbeh.2015.00309>.

- Duerden, E. G., M. Arsalidou, M. Lee, and M. J. Taylor. 2013. "Lateralization of Affective Processing in the Insula." *NeuroImage* 78: 159–175. <https://doi.org/10.1016/j.neuroimage.2013.04.014>.
- Eickhoff, S. B., K. E. Stephan, H. Mohlberg, et al. 2005. "A New SPM Toolbox for Combining Probabilistic Cytoarchitectonic Maps and Functional Imaging Data." *NeuroImage* 25, no. 4: 1325–1335. <https://doi.org/10.1016/j.neuroimage.2004.12.034>.
- Elliott, M. L., A. R. Knodt, D. Ireland, et al. 2020. "What Is the Test-Retest Reliability of Common Task-Functional MRI Measures? New Empirical Evidence and a Meta-Analysis." *Psychological Science* 31, no. 7: 792–806.
- Gaser, C., R. Dahnke, P. M. Thompson, F. Kurth, E. Luders, and Alzheimer's Disease Neuroimaging Initiative. 2024. "CAT—A Computational Anatomy Toolbox for the Analysis of Structural MRI Data." *Gigascience* 13: giae049. <https://doi.org/10.1093/gigascience/giae049>.
- Genauk, A., S. Quester, T. Wüstenberg, C. Mörsen, A. Heinz, and N. Romanczuk-Seiferth. 2017. "Reduced Loss Aversion in Pathological Gambling and Alcohol Dependence Is Associated With Differential Alterations in Amygdala and Prefrontal Functioning." *Scientific Reports* 7, no. 1: 16306.
- Gennatas, E. D., B. B. Avants, D. H. Wolf, et al. 2017. "Age-Related Effects and Sex Differences in Gray Matter Density, Volume, Mass, and Cortical Thickness From Childhood to Young Adulthood." *Journal of Neuroscience* 37, no. 20: 5065–5073. <https://doi.org/10.1523/JNEUROSCI.3550-16.2017>.
- Gianelli, C., G. Basso, M. Manera, P. Poggi, and N. Canessa. 2022. "Posterior Fronto-Medial Atrophy Reflects Decreased Loss Aversion, but Not Executive Impairment, in Alcohol Use Disorder." *Addiction Biology* 27, no. 1: e13088.
- Gorrino, I., N. Canessa, and G. Mattavelli. 2023. "Testing the Effect of High-Definition Transcranial Direct Current Stimulation of the Insular Cortex to Modulate Decision-Making and Executive Control." *Frontiers in Behavioral Neuroscience* 17: 1234837. <https://doi.org/10.3389/fnbeh.2023.1234837>.
- Gregory, M. D., J. S. Kippenhan, D. Dickinson, et al. 2016. "Regional Variations in Brain Gyriification Are Associated With General Cognitive Ability in Humans." *Current Biology* 26, no. 10: 1301–1305. <https://doi.org/10.1016/j.cub.2016.03.021>.
- Grill, F., L. Nyberg, and A. Rieckmann. 2021. "Neural Correlates of Reward Processing: Functional Dissociation of Two Components Within the Ventral Striatum." *Brain and Behavior: A Cognitive Neuroscience Perspective* 11, no. 2: e01987.
- Groman, S. M., C. Keistler, A. J. Keip, et al. 2019. "Orbitofrontal Circuits Control Multiple Reinforcement-Learning Processes." *Neuron* 103, no. 4: 734–746.
- Gu, X., and T. H. B. FitzGerald. 2014. "Interoceptive Inference: Homeostasis and Decision-Making." *Trends in Cognitive Sciences* 18, no. 6: 269–270. <https://doi.org/10.1016/j.tics.2014.02.001>.
- Gupta, C. N., J. A. Turner, and V. D. Calhoun. 2019. "Source-Based Morphometry: A Decade of Covarying Structural Brain Patterns." *Brain Structure and Function* 224, no. 9: 3031–3044. <https://doi.org/10.1007/s00429-019-01969-8>.
- Hartley, C. A., and E. A. Phelps. 2012. "Anxiety and Decision-Making." *Biological Psychiatry* 72, no. 2: 113–118.
- Hatton, S. N., J. Lagopoulos, D. F. Hermens, S. L. Naismith, M. R. Bennett, and I. B. Hickie. 2012. "Correlating Anterior Insula Gray Matter Volume Changes in Young People With Clinical and Neurocognitive Outcomes: An MRI Study." *BMC Psychiatry* 12, no. 1: 45. <https://doi.org/10.1186/1471-244X-12-45>.
- Haufler, D., O. Liran, R. J. Buchanan, and D. Pare. 2022. "Human Anterior Insula Signals Saliency and Deviations From Expectations via Bursts of Beta Oscillations." *Journal of Neurophysiology* 128, no. 1: 160–180. <https://doi.org/10.1152/jn.00106.2022>.
- Hegarty, A. K., M. S. Yani, A. Albishi, L. A. Michener, and J. J. Kutch. 2020. "Saliency Network Functional Connectivity Is Spatially Heterogeneous Across Sensorimotor Cortex in Healthy Humans." *NeuroImage* 221: 117177. <https://doi.org/10.1016/j.neuroimage.2020.117177>.
- Herman, A. M., G. Esposito, and M. Tsakiris. 2021. "Body in the Face of Uncertainty: The Role of Autonomic Arousal and Interoception in Decision-Making Under Risk and Ambiguity." *Psychophysiology* 58, no. 8: e13840.
- Himberg, J., A. Hyvärinen, and F. Esposito. 2004. "Validating the Independent Components of Neuroimaging Time Series via Clustering and Visualization." *NeuroImage* 22, no. 3: 1214–1222. <https://doi.org/10.1016/j.neuroimage.2004.03.027>.
- Hu, K., E. D. Rosa, and A. K. Anderson. 2024. "Attentional Priority and Limbic Activity Favor Gains Over Losses." *Neuroscience*. <https://doi.org/10.1101/2024.08.12.607518>.
- Im, K., J. Lee, U. Yoon, et al. 2006. "Fractal Dimension in Human Cortical Surface: Multiple Regression Analysis With Cortical Thickness, Sulcal Depth, and Folding Area." *Human Brain Mapping* 27, no. 12: 994–1003. <https://doi.org/10.1002/hbm.20238>.
- Jalon, I., A. Berger, B. Shofty, et al. 2023. "Lesions to Both Somatic and Affective Pain Pathways Lead to Decreased Saliency Network Connectivity." *Brain* 146, no. 5: 2153–2162. <https://doi.org/10.1093/brain/awac403>.
- Jauhar, S., L. Fortea, A. Solanes, A. Albajes-Eizagirre, P. J. McKenna, and J. Radua. 2021. "Brain Activations Associated With Anticipation and Delivery of Monetary Reward: A Systematic Review and Meta-Analysis of fMRI Studies." *PLoS One* 16, no. 8: e0255292.
- Jerčić, P., and V. Sundstedt. 2019. "Practicing Emotion-Regulation Through Biofeedback on the Decision-Making Performance in the Context of Serious Games: A Systematic Review." *Entertainment Computing* 29: 75–86. <https://doi.org/10.1016/j.entcom.2019.01.001>.
- Kahneman, D., and A. Tversky. 1979. "Prospect Theory: An Analysis of Decision Under Risk." *Econometrica* 47, no. 2: 263. <https://doi.org/10.2307/1914185>.
- Koffarnus, M. N., and B. A. Kaplan. 2018. "Clinical Models of Decision Making in Addiction." *Pharmacology Biochemistry and Behavior* 164: 71–83.
- Kohn, N., S. B. Eickhoff, M. Scheller, A. R. Laird, P. T. Fox, and U. Habel. 2014. "Neural Network of Cognitive Emotion Regulation—An ALE Meta-Analysis and MACM Analysis." *NeuroImage* 87: 345–355. <https://doi.org/10.1016/j.neuroimage.2013.11.001>.
- Krawczyk, D. C., and M. D'Esposito. 2013. "Modulation of Working Memory Function by Motivation Through Loss-Aversion." *Human Brain Mapping* 34, no. 4: 762–774. <https://doi.org/10.1002/hbm.21472>.
- Kutlu, M. G., J. E. Zachry, P. R. Melugin, et al. 2021. "Dopamine Release in the Nucleus Accumbens Core Signals Perceived Saliency." *Current Biology* 31, no. 21: 4748–4761.
- Lamballais, S., E. J. Vinke, M. W. Vernooij, M. A. Ikram, and R. L. Muetzel. 2020. "Cortical Gyriification in Relation to Age and Cognition in Older Adults." *NeuroImage* 212: 116637. <https://doi.org/10.1016/j.neuroimage.2020.116637>.
- Lavan, N., G. Rankin, N. Lorking, S. Scott, and C. McGettigan. 2017. "Neural Correlates of the Affective Properties of Spontaneous and Volitional Laughter Types." *Neuropsychologia* 95: 30–39. <https://doi.org/10.1016/j.neuropsychologia.2016.12.012>.
- LeDoux, J. 2012. "Rethinking the Emotional Brain." *Neuron* 73, no. 4: 653–676. <https://doi.org/10.1016/j.neuron.2012.02.004>.
- Li, C., X.-Q. Wang, C.-H. Wen, and H. Tan. 2020. "Association of Degree of Loss Aversion and Grey Matter Volume in Superior Frontal Gyrus

- by Voxel-Based Morphometry." *Brain Imaging and Behavior* 14, no. 1: 89–99. <https://doi.org/10.1007/s11682-018-9962-5>.
- Linhartová, P., A. Látalová, B. Kóša, T. Kašpárek, C. Schmahl, and C. Paret. 2019. "fMRI Neurofeedback in Emotion Regulation: A Literature Review." *NeuroImage* 193: 75–92. <https://doi.org/10.1016/j.neuroimage.2019.03.011>.
- Luders, E., P. M. Thompson, K. L. Narr, A. W. Toga, L. Jancke, and C. Gaser. 2006. "A Curvature-Based Approach to Estimate Local Gyrfication on the Cortical Surface." *NeuroImage* 29, no. 4: 1224–1230. <https://doi.org/10.1016/j.neuroimage.2005.08.049>.
- Markett, S., G. Heeren, C. Montag, B. Weber, and M. Reuter. 2016. "Loss Aversion Is Associated With Bilateral Insula Volume. A Voxel Based Morphometry Study." *Neuroscience Letters* 619: 172–176. <https://doi.org/10.1016/j.neulet.2016.03.029>.
- Mattavelli, G., S. Lo Presti, D. Tornaghi, and N. Canessa. 2022. "High-Definition Transcranial Direct Current Stimulation of the Dorsal Anterior Cingulate Cortex Modulates Decision-Making and Executive Control." *Brain Structure and Function* 227, no. 5: 1565–1576. <https://doi.org/10.1007/s00429-022-02456-3>.
- Mattavelli, G., T. J. Andrews, A. U. R. Asghar, J. R. Towler, and A. W. Young. 2012. "Response of Face-Selective Brain Regions to Trustworthiness and Gender of Faces." *Neuropsychologia* 50, no. 9: 2205–2211. <https://doi.org/10.1016/j.neuropsychologia.2012.05.024>.
- McDonough, I. M., and C. R. Madan. 2021. "Structural Complexity Is Negatively Associated With Brain Activity: A Novel Multimodal Test of Compensation Theories of Aging." *Neurobiology of Aging* 98: 185–196. <https://doi.org/10.1016/j.neurobiolaging.2020.10.023>.
- Mechelli, A., C. Price, K. Friston, and J. Ashburner. 2005. "Voxel-Based Morphometry of the Human Brain: Methods and Applications." *Current Medical Imaging Reviews* 1, no. 2: 105–113. <https://doi.org/10.2174/1573405054038726>.
- Menon, V., and L. Q. Uddin. 2010. "Saliency, Switching, Attention and Control: A Network Model of Insula Function." *Brain Structure and Function* 214, no. 5–6: 655–667. <https://doi.org/10.1007/s00429-010-0262-0>.
- Meregalli, V., F. Alberti, C. R. Madan, et al. 2022. "Cortical Complexity Estimation Using Fractal Dimension: A Systematic Review of the Literature on Clinical and Nonclinical Samples." *European Journal of Neuroscience* 55, no. 6: 1547–1583. <https://doi.org/10.1111/ejn.15631>.
- Molins, F., and M. A. Serrano. 2019. "The Neural Bases of Loss Aversion in Economic Contexts: A Systematic Review According to the PRISMA Guidelines." *Revista de Neurologia* 68, no. 2: 47–58.
- Mustafa, N., T. S. Ahearn, G. D. Waiter, A. D. Murray, L. J. Whalley, and R. T. Staff. 2012. "Brain Structural Complexity and Life Course Cognitive Change." *NeuroImage* 61, no. 3: 694–701. <https://doi.org/10.1016/j.neuroimage.2012.03.088>.
- Nicastro, N., M. Malpetti, E. Mak, et al. 2020. "Gray Matter Changes Related to Microglial Activation in Alzheimer's Disease." *Neurobiology of Aging* 94: 236–242. <https://doi.org/10.1016/j.neurobiolaging.2020.06.010>.
- Pareek, V., V. S. Rallabandi, and P. K. Roy. 2018. "A Correlational Study Between Microstructural White Matter Properties and Macrostructural Gray Matter Volume Across Normal Ageing: Conjoint DTI and VBM Analysis." *Magnetic Resonance Insights* 11: 1178623X18799926.
- Paulus, M. P., and J. L. Stewart. 2014. "Interoception and Drug Addiction." *Neuropharmacology* 76: 342–350.
- Pessiglione, M., and M. R. Delgado. 2015. "The Good, the Bad and the Brain: Neural Correlates of Appetitive and Aversive Values Underlying Decision Making." *Current Opinion in Behavioral Sciences* 5: 78–84. <https://doi.org/10.1016/j.cobeha.2015.08.006>.
- Pinger, M., J. Thome, P. Halli, W. H. Sommer, G. Koppe, and P. Kirsch. 2022. "Comparing Discounting of Potentially Real Rewards and Losses by Means of Functional Magnetic Resonance Imaging." *Frontiers in Systems Neuroscience* 16: 867202. <https://doi.org/10.3389/fnsys.2022.867202>.
- Pleger, B., and A. Villringer. 2013. "The Human Somatosensory System: From Perception to Decision Making." *Progress in Neurobiology* 103: 76–97. <https://doi.org/10.1016/j.pneurobio.2012.10.002>.
- Ploghaus, A., I. Tracey, J. S. Gati, et al. 1999. "Dissociating Pain From Its Anticipation in the Human Brain." *Science* 284, no. 5422: 1979–1981. <https://doi.org/10.1126/science.284.5422.1979>.
- Poppa, T., and A. Bechara. 2018. "The Somatic Marker Hypothesis: Revisiting the Role of the 'Body-Loop' in Decision-Making." *Current Opinion in Behavioral Sciences* 19: 61–66. <https://doi.org/10.1016/j.cobeha.2017.10.007>.
- Preuschoff, K., P. Bossaerts, and S. R. Quartz. 2006. "Neural Differentiation of Expected Reward and Risk in Human Subcortical Structures." *Neuron* 51, no. 3: 381–390. <https://doi.org/10.1016/j.neuron.2006.06.024>.
- Rick, S. 2011. "Losses, Gains, and Brains: Neuroeconomics Can Help to Answer Open Questions About Loss Aversion." *Journal of Consumer Psychology* 21, no. 4: 453–463. <https://doi.org/10.1016/j.jcps.2010.04.004>.
- Rolls, E. T. 2019. "The Orbitofrontal Cortex and Emotion in Health and Disease, Including Depression." *Neuropsychologia* 128: 14–43. <https://doi.org/10.1016/j.neuropsychologia.2017.09.021>.
- Rolls, E. T., W. Cheng, and J. Feng. 2020. "The Orbitofrontal Cortex: Reward, Emotion and Depression." *Brain Communications* 2, no. 2: fcaa196. <https://doi.org/10.1093/braincomms/fcaa196>.
- Romo, R., L. Lemus, and V. De Lafuente. 2012. "Sense, Memory, and Decision-Making in the Somatosensory Cortical Network." *Current Opinion in Neurobiology* 22, no. 6: 914–919. <https://doi.org/10.1016/j.conb.2012.08.002>.
- Rudebeck, P. H., and E. L. Rich. 2018. "Orbitofrontal Cortex." *Current Biology* 28, no. 18: R1083–R1088.
- Ruggeri, K., S. Alí, M. L. Berge, et al. 2020. "Replicating Patterns of Prospect Theory for Decision Under Risk." *Nature Human Behaviour* 4, no. 6: 622–633. <https://doi.org/10.1038/s41562-020-0886-x>.
- Samanez-Larkin, G. R., N. G. Hollon, L. L. Carstensen, and B. Knutson. 2008. "Individual Differences in Insular Sensitivity During Loss Anticipation Predict Avoidance Learning." *Psychological Science* 19, no. 4: 320–323. <https://doi.org/10.1111/j.1467-9280.2008.02087.x>.
- Schaefer, A., R. Kong, E. M. Gordon, et al. 2018. "Local-Global Parcellation of the Human Cerebral Cortex From Intrinsic Functional Connectivity MRI." *Cerebral Cortex* 28, no. 9: 3095–3114. <https://doi.org/10.1093/cercor/bhx179>.
- Schlund, M. W., G. J. Siegle, C. D. Ladouceur, et al. 2010. "Nothing to Fear? Neural Systems Supporting Avoidance Behavior in Healthy Youths." *NeuroImage* 52, no. 2: 710–719. <https://doi.org/10.1016/j.neuroimage.2010.04.244>.
- Schulreich, S., H. Gerhardt, D. Meshi, and H. R. Heekeren. 2020. "Fear-Induced Increases in Loss Aversion Are Linked to Increased Neural Negative-Value Coding." *Social Cognitive and Affective Neuroscience* 15, no. 6: 661–670. <https://doi.org/10.1093/scan/nsaa091>.
- Schulz, S. M. 2016. "Neural Correlates of Heart-Focused Interoception: A Functional Magnetic Resonance Imaging Meta-Analysis." *Philosophical Transactions of the Royal Society B: Biological Sciences* 371, no. 1708: 20160018.
- Serra, D. 2021. "Decision-Making: From Neuroscience to Neuroeconomics—An Overview." *Theory and Decision* 91, no. 1: 1–80.
- Singh, M. K. 2023. "Reproducibility and Reliability of Computing Models in Segmentation and Volumetric Measurement of Brain." *Annals of Neurosciences* 30, no. 4: 224–229. <https://doi.org/10.1177/09727531231159959>.

- Smith, C. D., H. Chebrolu, D. R. Wekstein, F. A. Schmitt, and W. R. Markesbery. 2007. "Age and Gender Effects on Human Brain Anatomy: A Voxel-Based Morphometric Study in Healthy Elderly." *Neurobiology of Aging* 28, no. 7: 1075–1087. <https://doi.org/10.1016/j.neurobiolaging.2006.05.018>.
- Sokol-Hessner, P., and R. B. Rutledge. 2019. "The Psychological and Neural Basis of Loss Aversion." *Current Directions in Psychological Science* 28, no. 1: 20–27. <https://doi.org/10.1177/0963721418806510>.
- Sokol-Hessner, P., C. A. Hartley, J. R. Hamilton, and E. A. Phelps. 2015. "Interoceptive Ability Predicts Aversion to Losses." *Cognition and Emotion* 29, no. 4: 695–701. <https://doi.org/10.1080/02699931.2014.925426>.
- Sokol-Hessner, P., C. F. Camerer, and E. A. Phelps. 2013. "Emotion Regulation Reduces Loss Aversion and Decreases Amygdala Responses to Losses." *Social Cognitive and Affective Neuroscience* 8, no. 3: 341–350. <https://doi.org/10.1093/scan/nss002>.
- Sokol-Hessner, P., M. Hsu, N. G. Curley, M. R. Delgado, C. F. Camerer, and E. A. Phelps. 2009. "Thinking Like a Trader Selectively Reduces Individuals' Loss Aversion." *Proceedings of the National Academy of Sciences of the United States of America* 106, no. 13: 5035–5040. <https://doi.org/10.1073/pnas.0806761106>.
- Stellern, J., K. B. Xiao, E. Grennell, M. Sanches, J. L. Gowin, and M. E. Sloan. 2023. "Emotion Regulation in Substance Use Disorders: A Systematic Review and Meta-Analysis." *Addiction* 118, no. 1: 30–47.
- Tan, Y., R. Yan, Y. Gao, M. Zhang, and G. Northoff. 2022. "Spatial-Topographic Nestedness of Interoceptive Regions Within the Networks of Decision Making and Emotion Regulation: Combining ALE Meta-Analysis and MACM Analysis." *NeuroImage* 260: 119500. <https://doi.org/10.1016/j.neuroimage.2022.119500>.
- Tanaka, S. C., K. Yamada, H. Yoneda, and F. Ohtake. 2014. "Neural Mechanisms of Gain-Loss Asymmetry in Temporal Discounting." *Journal of Neuroscience* 34, no. 16: 5595–5602. <https://doi.org/10.1523/JNEUROSCI.5169-12.2014>.
- Ter Harmel, J. F., M. L. Noordzij, A. E. Goudriaan, et al. 2021. "Biocueing and Ambulatory Biofeedback to Enhance Emotion Regulation: A Review of Studies Investigating Non-Psychiatric and Psychiatric Populations." *International Journal of Psychophysiology* 159: 94–106. <https://doi.org/10.1016/j.ijpsycho.2020.11.009>.
- Thiele, M., K. S. L. Yuen, A. V. Gerlicher, and R. Kalisch. 2021. "A Ventral Striatal Prediction Error Signal in Human Fear Extinction Learning." *NeuroImage* 229: 117709.
- Tom, S. M., C. R. Fox, C. Trepel, and R. A. Poldrack. 2007. "The Neural Basis of Loss Aversion in Decision-Making Under Risk." *Science* 315, no. 5811: 515–518. <https://doi.org/10.1126/science.1134239>.
- Uddin, L. Q., J. S. Nomi, B. Hébert-Seropian, J. Ghaziri, and O. Boucher. 2017. "Structure and Function of the Human Insula." *Journal of Clinical Neurophysiology* 34, no. 4: 300–306. <https://doi.org/10.1097/WNP.0000000000000377>.
- Ursu, S., and C. S. Carter. 2005. "Outcome Representations, Counterfactual Comparisons and the Human Orbitofrontal Cortex: Implications for Neuroimaging Studies of Decision-Making." *Cognitive Brain Research* 23, no. 1: 51–60. <https://doi.org/10.1016/j.cogbrainres.2005.01.004>.
- Verdejo-Garcia, A., L. Clark, and B. D. Dunn. 2012. "The Role of Interoception in Addiction: A Critical Review." *Neuroscience & Biobehavioral Reviews* 36, no. 8: 1857–1869. <https://doi.org/10.1016/j.neubiorev.2012.05.007>.
- Vignando, M., M. Aiello, A. Rinaldi, et al. 2019. "Food Knowledge Depends Upon the Integrity of Both Sensory and Functional Properties: A VBM, TBSS and DTI Tractography Study." *Scientific Reports* 9, no. 1: 7439.
- Wang, X., Q. Wu, L. Egan, et al. 2019. "Anterior Insular Cortex Plays a Critical Role in Interoceptive Attention." *eLife* 8: e42265. <https://doi.org/10.7554/eLife.42265>.
- Weibler, R. D., H. Berg, K. Fhong, et al. 2021. "The Neurobiology of Human Fear Generalization: Meta-Analysis and Working Neural Model." *Neuroscience & Biobehavioral Reviews* 128: 421–436. <https://doi.org/10.1016/j.neubiorev.2021.06.035>.
- Xiao, D., J. Li, Z. Ren, et al. 2024. "Association of Cortical Morphology, White Matter Hyperintensity, and Glymphatic Function in Frontotemporal Dementia Variants." *Alzheimer's & Dementia* 20, no. 9: 6045–6059. <https://doi.org/10.1002/alz.14158>.
- Xu, L., K. M. Groth, G. Pearlson, D. J. Schretlen, and V. D. Calhoun. 2009. "Source-Based Morphometry: The Use of Independent Component Analysis to Identify Gray Matter Differences With Application to Schizophrenia." *Human Brain Mapping* 30, no. 3: 711–724. <https://doi.org/10.1002/hbm.20540>.
- Xu, P., N. T. Van Dam, M. J. van Tol, et al. 2020. "Amygdala–Prefrontal Connectivity Modulates Loss Aversion Bias in Anxious Individuals." *NeuroImage* 218: 116957.
- Yotter, R. A., G. Ziegler, P. M. Thompson, and C. Gaser. 2011. "Diffeometric Anatomical Registration on the Surface [Poster]." Poster presented at the 7th Annual Meeting of the Organization for Human Brain Mapping.
- Yotter, R. A., I. Nenadic, G. Ziegler, P. M. Thompson, and C. Gaser. 2011. "Local Cortical Surface Complexity Maps From Spherical Harmonic Reconstructions." *NeuroImage* 56, no. 3: 961–973. <https://doi.org/10.1016/j.neuroimage.2011.02.007>.
- Yotter, R. A., P. M. Thompson, and C. Gaser. 2011. "Algorithms to Improve the Reparameterization of Spherical Mappings of Brain Surface Meshes." *Journal of Neuroimaging* 21, no. 2: e134–e147. <https://doi.org/10.1111/j.1552-6569.2010.00484.x>.
- Yotter, R. A., R. Dahnke, P. M. Thompson, and C. Gaser. 2011. "Topological Correction of Brain Surface Meshes Using Spherical Harmonics." *Human Brain Mapping* 32, no. 7: 1109–1124. <https://doi.org/10.1002/hbm.21095>.
- Zha, R., J. Bu, Z. Wei, et al. 2019. "Transforming Brain Signals Related to Value Evaluation and Self-Control Into Behavioral Choices." *Human Brain Mapping* 40, no. 4: 1049–1061. <https://doi.org/10.1002/hbm.24379>.

Supporting Information

Additional supporting information can be found online in the Supporting Information section.